A systematic study on the preparation and hydrogen storage of Zeolite 13X templated microporous carbons

Zhuxian Yang,[a] Wei Xiong,[b] Yanqiu Zhu,[a] and Yongde Xia*[a]

[a] College of Engineering, Mathematics and Physical Sciences, University of Exeter, Exeter EX4 4QF, United Kingdom

[b] School of Chemistry and Chemical Engineering, Chongqing University of Science and Technology, Chongqing, P. R. China

Email: y.xia@exeter.ac.uk; Homepage: http://emps.exeter.ac.uk/engineering/staff/yx236

ABSTRACT

We present a systematic study on the CVD-based synthesis strategies (single CVD process, two CVD process and combination of liquid impregnation and CVD process) for the nanocasting of zeolite-templated porous carbon materials using commercially available zeolite 13X as the hard template, and ethylene, furfuryl alcohol, acetonitrile and/or vinylcyanide as carbon precursors. The results indicate that the combination of liquid impregnation and CVD process is superior to the single CVD process or the two CVD process in producing carbon materials with high surface area, high pore volume and high level of microporosity. The combination of liquid impregnation with furfuryl alcohol and CVD with ethylene generates carbon materials with the highest surface area of 2841 m^2/g, pore volume of 1.54 cm^3/g and hydrogen uptake capacity of 6.3 wt% (at -196 °C and 20 bar). Under the studied conditions, the porous carbon materials exhibit variable structural ordering and tuneable textural properties with surface area of 1600 – 2850 m^2/g, pore volume of 1.0 – 1.8 cm^3/g, and hydrogen uptake capacity in the range of 3.4 – 6.3 wt% (at -196 ^oC and 20 bar). Notably, a linear relationship between the hydrogen uptake capacity and the total surface area, and the micropore volume, and the micropore surface area respectively is found for the studied porous carbons, implying the important role of the total surface area, the micropore volume and the micropore surface area in the hydrogen adsorption.

Keywords: Microporous carbon / Zeolite 13X / CVD / Hydrogen storage

Introduction

Porous carbon materials with well-ordered pore systems have potential applications in catalysis, molecular sieving, as components of electrochemical devices or as gas storage media due to their remarkable properties,[1] such as high surface area, high pore volume, chemical inertness, easy handling and low cost of manufacture.[2] Therefore, much effort has been devoted to the synthesis of ordered porous carbon materials.[2-3] The template carbonisation method has been extensively studied and demonstrated as one of the most effective approaches for the fabrication of porous carbon materials, which allows the control over the properties of the resulting carbon materials with tailored physical and chemical properties.[2-3]

So far a variety of templates, including microporous zeolites, mesoporous silica or aluminosilicates, metal-organic frameworks (MOFs) and colloids have been used to prepare porous carbons.[2-3] Among them, zeolites are attractive due to their versatility and three-dimensional pore channels, and the resulting templated carbons usually possess high surface area and pore volume along with significant levels of microporosity,[3a, 3b, 4] which is expected to be beneficial for hydrogen storage.[4f] A large number of zeolites with a variety of pore structures have been used as hard templates for the synthesis of high surface area carbons,[3a, 3b, 4a-g, 5] however, only a few of them can transfer their structural ordering to the porous carbon replicas.[4a, 4b, 4d, 4e, 5-6] It has been suggested that the poor replication of the zeolite structure in carbons is due to the small pore size of zeolites which results in low carbon loading, or disorder/inappropriate symmetry of the zeolite pore ordering.[3b, 4d] In this regard, Parmentier and co-workers have used a large pore zeolite with a two- or three-dimensional noncubic pore system (e.g., zeolite EMC-2) as template and succeeded in preparing a zeolite carbon replica with more than one XRD peak.[4d] Apart from the nature of the zeolite template, it has been reported that the synthesis route also play a significant role in determining the structural regularity and textural properties of the zeolite templated carbons.[4d, 5, 7] For example, the two-

step method by combining liquid impregnation of furfuryl alcohol and CVD of another carbon precusor has been demonstrated to increase the carbon loading and consequently the structural ordering of the resulting carbon.[4c] To date, there have been a few reports on the synthesis of porous carbon and the hydrogen storage properties using zeolite 13X as the template,[4h, 8] however, there has been no systematic studies on the preparation of porous carbon materials using zeolite 13X as template.

In this report, nanocasting of templated porous carbon materials via CVD-based synthesis strategies using commercially available zeolite 13X as the template have been systematically investigated. The effect of varying the nature of carbon precursors, the way of carbon precursor been introduced into the template pores, and the influence of using a two-step process involving either two CVD steps or a combination of liquid impregnation and CVD, and a further heat treatment of the carbonized carbon/template composite have been studied. Moreover, the hydrogen uptake capacity of the resulting templated porous carbons have been evaluated and discussed with respect to their textural properties.

Results and Discussion

The templated carbon materials synthesised via CVD-based strategies are summarised in Table 1. Figure 1A shows the powder X-ray diffraction (XRD) patterns of the zeolite 13X and corresponding templated carbons obtained by using ethylene or acetonitrile as the single carbon precusor. The XRD patterns of all three samples CXET, CXETD and CXETS derived from ethylene show a peak, similar to that present in the zeolite 13X, at ca. 2θ = 6.3 °, indicating that the resulting carbon materials exhibit some structural ordering similar to that of the zeolite 13X template. Sample CXETS shows the peak with the highest intensity and sharpness implying that single CVD process followed by a short heat treatment (sample CXETS) leads to carbon with the highest zeolite structural ordering compared wtih the two

CVD pocess followed by heat treatment (sample CXETD), and single CVD process followed by heat treatment (sample CXET). In addition, no diffraction peak at 2θ of 26 ^{o} (the (002) diffraction for graphitic carbon) can be observed for all three carbon materials, suggesting that the carbons are amorphous (i.e., non-graphitic). However, for the acetonitrile derived sample CXAN, the peak at ca. 2θ = 6.3 ° is invisible showing that no srtuctual ordering of the zeolite 13X template has been replicated in the carbon; while the presence of a broad peak at 2θ of 26^{o} suggests some extent of graphitisation of the carbon. The difference in the srtuctual ordering between the ethylene-derived carbon and the acetonitrile-derived one could be explained as follows. As disscussed previously that during the carbonisation process (pyrolysis and CVD), the high temperature used accelerates the formation of carbon on and within the surface/near surface region of the zeolite pore channels. The accelerated carbonisation process results in the deposition of carbon particles mainly into the pore regions close to the outer surface (i.e., pore mouth) of the zeolite particle.[8d] In the case of ethylene, the molecular size is relatively small, it can diffuse into the zeolite pore channel and lead to the replication of zeolite structural ordering in the resulting carbons. However, the molecular size of acetonitrile is larger than that of ethylene, the diffusion rate is relatively slow and it is difficult for it to diffuse into the zeolite pore channel due to pore blocking by already deposited carbon, which results in the formation of carbon partly on the outer surface of the zeolite particles. In this case, the growth of graphitic carbon is not limited by the spacial limitations of the zeolite channels. The sum effect of the pore blocking and the partly carbonisation on the outer surface of the zeolite particles results in poor replication of zeolite structural ordering in the resulting carbons yet some extent graphitisation of the carbons.

The nitrogen sorption isotherms of the resulting carbon materials and that of the zeolite template 13X are shown in Figure 1B. All the isotherms exhibit some adsorption below *P*/*P*o = 0.2, which may be ascribed to micropore filling. The isotherms of carbon samples also exhibit

nitrogen uptake at $P/P_o > 0.2$, which may be attributed to adsorption into mesopores arising from interparticle voids. As shown in Table 1, CXET gives higher surface area and pore volume compared to that of CXETS (short heat tratment), suggesting that 3 h heat treatment of the zeolite/carbon composite is better. In additon, sample CXETD (via two CVD process) exhibits the lowest textural data compared with the other two ethylene-derived carbons (CXET and CXETS). An attempted explanation might be as follows, the first CVD process at 650 °C could result in the full occupation of the pore channels by deposited carbon and consequently hinders further introduction of carbon precusors into the pore channels during the second CVD process at 700 °C. As a result, the carbon could mainly be produced by the first CVD process at 650 °C, and the second CVD process at 700 °C plays little role, which results in carbons with textual data similar to carbons produced by a single CVD process at 650 °C. In addition, the textual data of the ethylene-derived carbons are generally higher than those of the acetonitrile derived carbon (CXAN), and the ethylene-derived carbons show structual ordering replicated from the zeolite 13X template while the acetonitrile-derived carbon does not, suggesting that for single CVD procedure ethylene is a better carbon precusor in producing carbons with high surface area and pore volumes while retaining some structural ordering of the zeolite 13X template. On the other hand, the surface area of the acetonitrile derived carbon (CXAN) with a 3 h heat treatment of the zeolite/carbon composite in this study is 1602 m^2/g, of which 46% of the surface area and 0.29% of the pore volume is contributed from micropore. However, the surface area of the acetonitrile-derived carbon from previous study under the same CVD conditions except for without further heat treatment of the zeolite/carbon composite is only 1499 m^2/g with only 16% of the surface area and 9% of the pore volume contributed from micropore [8d]. As discussed in our previous paper,[9] this suggests that the heat treatment step is very important in improving both the total and microporous surface area and pore volume, which is benificail for hydrgoen storage.

In the combination of liquid impregnation and CVD process, furfuryl alcohol and vinylcyanide respectively was used as the carbon precusor for the liquid impregnation step, and ethylene and acetonitrile respectively for the CVD step. The XRD patterns of the two-step derived carbons are shown in Figure 2A. All the carbons obtained from ethylene as the carbon precusor in the CVD process regardless of the different carbon precusors used in the liquid impregnation step exhibit the peak at ca. 2θ = 6.3 °, implying that the zeolite structural ordering has been transferred to the resulting carbons. However, this peak can not be observed in the carbon derived with acetonitrile as the carbon precusor in the CVD step, suggesting that no zeolite structural ordering has been transferred to the resulting carbon. This indicates that the replication of zeolite-like structural ordering in carbons prepared via liquid impregnation combined with a CVD step depends on the carbon precursor used in the CVD step. As discussed above, once again, the molecular size of the carbon precusor in the CVD step plays the key role in the replicating of the zeolite structural ordering into the resulting carbon. This is in agreement with our previous report on zeilite Y being the template.[8d, 10] In addition, all the carbons show a neglegible broad peak at 2θ = 26 °, implying the amorphous nature of the carbons.

The nitrogen sorption isotherms of the two-step derived carbon materials are shown in Figure 2B. The isotherms of all the samples exhibit some adsorption below *P*/*P*o = 0.2, which may be ascribed to micropore filling. The isotherms of carbon samples also exhibit nitrogen uptake at *P*/*P*o > 0.2, which may be attributed to adsorption into mesopores arising from interparticle voids. The textural properties of the carbon materials summarised in Table 1 show that these two-step derived carbons exhibit surface area of 2174 - 2841 m^2/g and pore volume of 1.13 - 1.83 cm^3/g, generally higher than that of those carbons derived by single CVD. These values are comparable to those previously reported 13X-templated carbons.[4h, 11] Moreover, the level of microporosity of the two-step derived carbons is also generally higher than those of

carbons derived by single CVD. These results demonstrate that the two-step strategy is superior to the single CVD procedure in producing carbons with high surface area and pore volume and high level of microporosity. Sample CXFAETS, obtained using furfuryl alcohol as the carbon precursor in the liquid impregnation step and ethylene as the carbon precursor in the CVD procedure shows the highest surface area of 2841 m^2/g and level of microporosity (with 79% of the surface area and 62% of the pore volume contributed from micropore). The textual data of carbons CXFAET and CXVCET in Table 1 suggest that there is no difference between furfuryl alcohol and vinylcyanide as the carbon precursor in the liquid impregnation procedure. However, in the case of furfuryl alcohol as the carbon precursor in the liquid impregnation procedure, carbon CXFAET using ethylene as the carbon precursor in the CVD step exhibits higher surface area and pore volume than that of carbon CXFAAN using acetonitrile as the carbon precursor in the CVD step. This is similar to the results from single CVD process, suggesting that ethylene is superior to acetonitrile as the carbon precursor for high surface area and pore volume carbon production under studied conditions. Based on the above results, in some extent, the textural properties of carbons can be controlled by choosing the preparation strategies.

Raman spectroscopy is a useful tool for the characterisation of crystalline and amorphous carbons. Figure 3 shows the Raman spectra of samples CXETS, CAN, CXVCET, CXFAAN and CXFAET. The Raman spectra show two bands at ca. 1350 cm^{-1} (D band) and ca. 1580 cm^{-1} (G band). The D band is an indication of amorphous carbon or defects/ reduction in graphitic ordering, or it may arise from finite size effects in graphitic materials.[12] The G band is generally ascribed to the carbon-carbon stretching (E2g) mode for graphene sheets. As it has been noted that the G and D peaks of varying intensity, position and width dominate the Raman spectra of nanocrystalline and amorphous carbons, even those without widespread graphitic ordering.[13] Therefore, the low intensity and the broadness of the G band of all the

carbons in Figure 3 suggest they are all amorphous carbon, in good agreement with the XRD patterns shown in Figure 1A and Figure 2A.

The particle morphology was examined by scanning electron microscopy (SEM). Figure 4 shows the SEM images of the template zeolite 13X and some of the carbon materials. The zeolite 13X template shows sphere-like particles with size of 2 – 3 μm. All the carbon samples, prepared via various synthesis strategies, also show sphere-like particles of 2 – 3 μm. This suggests that the morphology of the zeolite 13X template is transferred to the resulting carbons. This is consistent with the templating mechanism whereby the carbon is predominantly nanocast within the pore channels of the zeolite 13X template. Figure 5 shows two representative transmission electron microscopy (TEM) images of carbons CXET and CXFAET, which shows a worm-like pore structure, indicating the replication is not very much perfect (as suggested by the XRD results in Figures 1A and 2A). The insert of the SAED patterns implies the amorphous nature of the carbons, again in agreement with the XRD results.

Due to the use of N-containing carbon precursor (acetonitrile and vinylcyanide), the resulting carbons show a nitrogen content of 7.22 wt% for CXFAAN, 9.16 wt% for CXAN and 0.25 wt% for CXVCET in Table 1. This result suggests that the nitrogen content of the carbon can be controlled by varying the carbon precursors and the synthesis strategy. Information on the nature of the binding between carbon and nitrogen in the N-doped carbons was obtained from X-ray photoelectron spectroscopy (XPS). Figure 6 shows the detailed C 1s and N 1s spectra. The C 1s peak for samples was centred at ca. 284.5 eV and showed a slightly asymmetric nature. The N 1s signal is split into two main peaks at 400.5 and 398.6 eV. The peak at 398.6 eV has previously been ascribed to defects within graphene sheets,[14] and the peak at ca. 400.5 eV is due to pyrrolic type N incorporated into graphene sheets.[15] The absence of the peak at ca. 403 eV due to so-called “graphitic” nitrogen, i.e., highly coordinated N atoms substituting

inner C atoms on the graphene layers[15b] suggests the amorphous nature of the carbons, in agreement with above XRD and Raman results.

The hydrogen uptake capacity of the porous carbon materials was measured gravimetrically at -196 °C over the pressure range of 0 – 20 bar. The hydrogen uptake isotherms are shown in Figure 7. No observable hysteresis in the hydrogen sorption isotherms for all the samples implies that the uptake of hydrogen is totally reversible. The hydrogen uptake capacities at 1 and 20 bar respectively, as summarised in Table 1, are in the range of 1.5 – 2.4 wt% at 1 bar and 3.5 – 6.3 wt% at 20 bar respectively. Carbon CXFAETS exhibits the highest uptake of 6.3 wt% while carbon CXETD shows the lowest uptake of 3.5 wt%. These uptake values are comparable to those reported for zeolite-templated carbon materials [4h, 5, 8d, 16]. Figure 7 also shows that the hydrogen uptake capacity is closely related to the textural properties of the carbon materials, especially the surface area. In particular, carbon CXFAETS with the highest total surface area and pore volume, and also the highest micropore surface area and volume, gives the highest hydrogen uptake capacity. A detailed examination of the link between the hydrogen sorption and the textural properties is presented in Figure 8. Apart from a close relationship between the uptake capacity (at 20 bar) and the total surface area (R = 0.964) and the micropore volume (R = 0.976) respectively can be derived, which is in good agreement with previous reports;[4e, 17] there is also a linear relationship between the hydrogen uptake capacity (at 20 bar) and the micropore surface area (R = 0.981), which to our best of knowledge has never been reported. There is, however, relatively poor relationship between the hydrogen uptake capacity at 20 bar and the total pore volume of the studied porous carbon materials (R=0.765). All these results clearly indicate the importance of the total surface area and the micropore volume as well as the micropore surface area in determining the hydrogen uptake capacity, which may provide guidance for the design of new-type porous carbon materials for high hydrogen storage.

It is worth pointing out that for practical applications, hydrogen storage at room temperature is more desirable than at -196 °C. However, physisorption of hydrogen by porous materials at room temperature are very low [18]. In this respect, there have been reports on the enhancement of hydrogen storage on adsorbents materials by hydrogen dissociation followed by spillover [19], yet the uptake values are still far below the amount required for practical applications requirement.

Conclusions

A systematic study on the CVD-based synthesis strategies for the nanocasting of porous carbon materials using commercially available zeolite 13X as the hard template, and ethylene, furfuryl alcohol, acetonitrile and/or vinylcyanide as carbon precursors has been presented. In both cases, i. e. the single CVD procedure and the two step strategy (combination of liquid impregnation with CVD process), ethylene is superior to acetonitrile as the carbon precursor in producing porous carbon with zeolite-structural ordering, high surface area and pore volume, and high level of microporosity. The two-step strategy produces carbons with higher textual properties than the single CVD procedure. The porous carbon materials exhibit variable structural ordering and tuneable textural properties with surface area of 1600 – 2850 m^2/g, pore volume of 1.0 – 1.8 cm^3/g, and hydrogen uptake capacity in the range of 3.4 – 6.3 wt% (at -196 ^oC and 20 bar). A linear relationship between the uptake capacity (at 20 bar) and the total surface area, the micropore volume, and the micropore surface area respectively is found for the carbons, which may help for the design of new-type porous carbon materials for high hydrogen storage.

Experimental Section

Material Synthesis: To obtain carbon materials, zeolite 13X was used as template and ethylene (ET), furfuryl alcohol (FA), acetonitrile (AN) and/or vinylcyanide (VC) as carbon precursors. Zeolite 13X was purchased from Fluka. Carbon samples were synthesised with ethylene as carbon precursor using single or two sequent chemical vapour deposition (CVD) steps. A typical synthesis method for carbons derived from ethylene was as follows: an alumina boat with 1 g of zeolite 13X was placed in a flow-through tube (with internal diameter of 25 mm) furnace. The furnace was heated to the required temperature (650 or 700 °C) under argon and then maintained for 3 h under ethylene gas (100 mL/min), followed either by further heat treatment in an argon atmosphere at 900 ^{o}C under different duration (sample designed as CXET was derived from zeolite 13X under 3 h heat treatment and the sample named as CXETS was under 1 h heat treatment), or by a second CVD step with ethylene (100 mL/min) at 700 ^{o}C for 3 h and finally subject to heat treatment in argon at 900 ^{o}C for 3 h (sample CXETD). After cooling down to room temperature under argon, the resulting zeolite/carbon composites were recovered and washed with 10% hydrofluoric (HF) acid several times, followed by refluxing at 60 °C in concentrated hydrochloric acid (HCl) for 6 h to completely remove the zeolite framework. Finally, the resulting carbon materials were dried in an oven at 120 °C overnight.

Two samples derived from acetonitrile were synthesised by single CVD method as follows; 1 g zeolite 13X in an alumina boat was placed in a flow through tube furnace. The furnace was heated to a target temperature of 800 ^{o}C under argon and then maintained for 3 h under argon saturated with acetonitrile (100 mL/min) to allow CVD of carbon into the zeolite. The gas flow was then switched to argon only and the temperature of the furnace was raised and maintained at 900 ^{o}C for 3 h. After cooling down to room temperature under argon, the resulting zeolite/carbon composites were recovered and washed with 10% hydrofluoric (HF) acid several times, followed by refluxing at 60 °C in concentrated hydrochloric acid (HCl) for

6 h, and dried at 120 ºC as described above. The obtained carbon samples were labeled as CXAN.

Four further carbon samples were prepared using a combination of liquid impregnation and CVD method as follows; 1 g of zeolite 13X previously dried in oven at 300 ºC, was impregnated with furfuryl alcohol, which was polymerised under argon at 80 ºC for 24 h and then at 150 ºC for 8 h followed by pyrolysis at 700 ºC under argon for 3 h. Then the composite was exposed to ethylene via CVD at 700 ºC for 1 h (sample CXFAETS) or 3 h (sample CXFAET) or exposed to argon saturated with acetonitrile via CVD at 800 ºC for 3 h (sample CXFAAN). The gas flow was then switched to argon only and the temperature of the furnace was increased to 900 ºC and maintained for 3 h. After cooling down to room temperature under argon, the carbon/zeolite composite was washed with HF and HCl, and dried as described above. A sample labeled as CXVCET was also prepared under the same conditions for the preparation of CXFAET except that vinylcyanide instead of furfuryl alcohol was used as the carbon precursor in the liquid impregnation step.

Material Characterisation: Powder XRD analysis was performed using a Philips Advanced D8 powder diffractometer with Cu Kα radiation (40 kV, 25 mA), 0.02° step size, and 2 s step time. Textural properties were determined via nitrogen sorption at -196 °C using a conventional volumetric technique on a Quantachrome Autosorb iQ sorptometer. Before analysis, the samples were evacuated for 12 h at 300 °C under vacuum. The surface area was calculated using the Brunauer-Emmett-Teller (BET) method based on adsorption data in the partial pressure (P/Po) range 0.02 – 0.22, and total pore volume was determined from the amount of nitrogen adsorbed at P/Po ca. 0.99. (We note that the BET method has limitations with respect to calculating the surface area of microporous materials, but is suitably used here for comparative analysis of the surface area of a set of microporous samples. The partial pressure range (P/Po) 0.02 – 0.22, for the calculation of surface area was selected taking into

account previous reports which indicate that using low partial pressure range *P*/*P*o 0.01 – 0.05, overestimates the surface area while using the partial pressure range *P*/*P*o 0.1 – 0.3 can underestimate the surface area).[4d] Micropore surface area and micropore volume were obtained via *t*-plot analysis. Elemental analysis was carried out using a CHNS analyser (Fishons EA 1108). Thermogravimetric analysis (TGA) was performed using a TA SDT Q600 instrument with a heating rate of 10 °C/min under flowing air. Scanning electron microscopy (SEM) images were recorded using a Philips XL-30 scanning electron microscope. Samples were mounted using a conductive carbon double-sided sticky tape. A thin (ca. 10 nm) coating of gold sputter was deposited onto the samples to reduce the effects of charging. Transmission electron microscopy (TEM) images were recorded on a JEOL 2000-FX electron microscope operating at 200 kV. Samples for analysis were prepared by dispersing carbon powder in acetone solvent, then dropping and spreading them on a holey carbon film supported on a grid. After vaporising the solvent, the dry carbon sample was retained on the grid. Raman spectra were obtained on a Nicolet Almega Dispersive Raman microscope with 532 nm. The Raman spectra were collected by manually placing the probe tip near the desired point of the sample on a glass slide at room temperature. X-ray photoelectron spectroscopy (XPS) was performed using a Kratos AXIS ULTRA spectrometer with a mono-chromated Al X-ray source (1486.6 eV) operated at 10 mA emission current and 15 kV anode potential. The analysis chamber pressure was better than 1.3×10^{-12} bar. The take-off angle for the photoelectron analyzer was 90°, and the acceptance angle was 30° (in magnetic lens modes).

Hydrogen Uptake Measurements: Gravimetric analysis of hydrogen uptake capacity was performed using high-purity hydrogen (99.9999%) over the pressure range 0 – 20 bar with an Intelligent Gravimetric Analyzer (IGA-003, Hiden), which incorporates a microbalance capable of measuring weights with a resolution of ±0.2 μg. The samples in the analysis chamber of the IGA-003 were evacuated to 10^{-10} bar and kept at 250 °C overnight before

measurement. The hydrogen uptake measurements were carried out at -196 °C in a liquid nitrogen bath. The high-purity hydrogen (99.9999%) was additionally purified by a molecular sieve filter and a liquid nitrogen trap.

Acknowledgements

The authors are grateful to the Royal Society, the Royal Academy of Engineering and Bayu Oversea Intelligence Plan of Chongqing for financial support.

References:

[1] a) A. C. Dillon, M. J. Heben, *Appl. Phys. A* **2001**, *72*, 133-142; b) M. Hirscher, B. Panella, *J. Alloys Compd.* **2005**, *404*, 399-401.

[2] B. Sakintuna, Y. Yurum, *Ind. Eng. Chem. Res.* **2005**, *44*, 2893-2902.

[3] a) T. Kyotani, *Carbon* **2000**, *38*, 269-286; b) T. Kyotani, Z. Ma, A. Tomita, *Carbon* **2003**, *41*, 1451-1459; c) R. Ryoo, S. H. Joo, M. Kruk, M. Jaroniec, *Adv. Mater.* **2001**, *13*, 677-681; d) J. Lee, J. Kim, T. Hyeon, *Adv. Mater.* **2006**, *18*, 2073-2094; e) J. M. Juarez, M. B. Gomez, O. A. Anunziata, *Int. J. Energy Res.* **2015**, *39*, 941-953; f) S. Dutta, A. Bhaumik, K. C. W. Wu, *Energy Environ. Sci.* **2014**, *7*, 3574-3592; g) Z. Yang, Y. Xia, Y. Zhu, *Mater. Chem. Phys.* **2013**, *141*, 318-323.

[4] a) Z. X. Ma, T. Kyotani, Z. Liu, O. Terasaki, A. Tomita, *Chem. Mater.* **2001**, *13*, 4413-4415; b) Z. X. Ma, T. Kyotani, A. Tomita, *Chem. Commun.* **2000**, 2365-2366; c) P. Hou, H. Orikasa, T. Yamazaki, K. Matsuoka, A. Tomita, N. Setoyama, Y. Fukushima, T. Kyotani, *Chem. Mater.* **2005**, *17*, 5187-5193; d) F. O. M. Gaslain, J. Parmentier, V. P. Valtchev, J. Patarin, *Chem. Commun.* **2006**, 991-993; e) Y. D. Xia, G. S. Walker, D. M. Grant, R. Mokaya, *J. Am. Chem. Soc.* **2009**, *131*, 16493-16499; f) A. Garsuch, O. Klepel, *Carbon* **2005**, *43*, 2330-2337; g) A. Garsuch, O. Klepel, R. R. Sattler, C. Berger, R. Glaeser, J. Weitkamp, *Carbon* **2006**, *44*, 593-596; h) E. Masika, R. Mokaya, *Prog. Nat. Sci. Mater. Int* **2013**, *23*, 308-316.

[5] Z. Yang, Y. Xia, R. Mokaya, *J. Am. Chem. Soc.* **2007**, *129*, 1673-1679.

[6] S. Lei, J. I. Miyamoto, T. Ohba, H. Kanoh, K. Kaneko, *J. Phys. Chem. C* **2007**, *111*, 2459-2464.

[7] C. Ducrot-Boisgontiera, J. Parmentier, J. Patarin, *Microporous Mesoporous Mater.* **2009**, *126*, 101-106

[8] a) H. Wang, Q. Gao, J. Hu, Z. Chen, *Carbon* **2009**, *47*, 2259-2268; b) H. L. Wang, Q. M. Gao, J. Hu, *Microporous Mesoporous Mater.* **2010**, *131*, 89-96; c) E. Masika, R. Mokaya, *J. Phys. Chem. C* **2012**, *116*, 25734-25740; d) Z. Yang, Y. Xia, X. Sun, R. Mokaya, *J. Phys. Chem. B* **2006**, *110*, 18424-18431.

[9] Y. Xia, Z. Yang, X. Gou, Y. Zhu, *Int. J. Hydrogen Energy* **2013**, *38*, 5039-5052.

[10] Y. D. Xia, Z. X. Yang, R. Mokaya, *Chem. Vap. Deposition* **2010**, *16*, 322-328.

[11] H. Wang, Q. Gao, J. Hu, *Microporous and Mesoporous Materials* **2010**, *131*, 89-96.

[12] a) F. Tuinstra, J. L. Koenig, *J. Chem. Phys.* **1970**, *53*, 1126-1130; b) A. A. Zakhidov, R. H. Baughman, Z. Iqbal, C. X. Cui, I. Khayrullin, S. O. Dantas, I. Marti, V. G. Ralchenko, *Science* **1998**, *282*, 897-901.

[13] A. C. Ferrari, J. Robertson, *Phys. Rev. B* **2000**, *61*, 14095-14107.

[14] a) R. Sen, B. C. Satishkumar, S. Govindaraj, K. R. Harikumar, M. K. Renganathan, C. N. R. Rao, *J. Mater. Chem.* **1997**, *7*, 2335-2337; b) M. Terrones, P. Redlich, N. Grobert, S. Trasobares, W. K. Hsu, H. Terrones, Y. Q. Zhu, J. P. Hare, C. L. Reeves, A. K. Cheetham, M. Ruhle, H. W. Kroto, D. R. M. Walton, *Adv. Mater.* **1999**, *11*, 655-658; c) W. H. Xu, T. Kyotani, B. K. Pradhan, T. Nakajima, A. Tomita, *Adv. Mater.* **2003**, *15*, 1087-1090; d) M. Terrones, N. Grobert, H. Terrones, *Carbon* **2002**, *40*, 1665-1684.

[15] a) J. M. J. Mateos, J. L. G. Fierro, *Surf. Interface Anal.* **1996**, *24*, 223-236; b) J. Casanovas, J. M. Ricart, J. Rubio, F. Illas, J. M. Jimenez-Mateos, *J. Am. Chem. Soc.* **1996**, *118*, 8071-8076.

[16] H. Nishihara, T. Kyotani, *Adv. Mater.* **2012**, *24*, 4473-4498.

[17] a) N. Texier-Mandoki, J. Dentzer, T. Piquero, S. Saadallah, P. David, C. Vix-Guterl, *Carbon* **2004**, *42*, 2744-2747; b) Y. Gogotsi, R. K. Dash, G. Yushin, T. Yildirim, G. Laudisio, J. E. Fischer, *J. Am. Chem. Soc.* **2005**, *127*, 16006-16007; c) X. B. Zhao, B. Xiao, A. J. Fletcher, K. M. Thomas, *J. Phys. Chem. B* **2005**, *109*, 8880-8888; d) B. Z. Fang, H. S. Zhou, I. Honma, *J. Phys. Chem. B* **2006**, *110*, 4875-4880.

[18] L. F. Wang, R. T. Yang, *J. Phys. Chem. C* **2009**, *113*, 21883-21888.

[19] a) Z. Wang, F. H. Yang, R. T. Yang, *J. Phys. Chem. C* **2010**, *114*, 1601-1609; b) L. Wang, R. T. Yang, *J. Phys. Chem. C* **2008**, *112*, 12486-12494.

Table 1 Textural properties, elemental composition, and hydrogen uptake capacity of microporous carbon templated from Zeolite 13X

sample	Synthesis conditions	N content (wt %)	Surface area (m^2/g)[a]	Pore volume (cm^3/g)[b]	Hydrogen uptake (wt %)[c,d]
13X			723	0.35	
CXETD	C_2H_4 650 °C/3 h + C_2H_4 700 °C/3 h + HT		1670 (1177)	0.93 (0.49)	3.48 (1.54)
CXET	C_2H_4 700 °C/3 h + HT		2466 (1686)	1.41 (0.69)	5.13 (1.99)
CXETS	C_2H_4 700 °C/3 h + HT-S		2194 (1589)	1.18 (0.65)	4.44 (1.67)
CXFAETS	FA polymerized + C_2H_4 700 °C/1 h + HT		2841 (2242)	1.54 (0.95)	6.26 (2.36)
CXFAET	FA polymerized + C_2H_4 700 °C/3 h + HT		2568 (1802)	1.42 (0.74)	5.11 (1.90)
CXFAAN	FA polymerized + CH_3CN 800 °C/3 h + HT	7.22	2174 (1672)	1.13 (0.70)	4.90 (2.16)
CXVCET	VC polymerized + C_2H_4 700 °C/3 h + HT	0.25	2572 (1711)	1.83 (0.71)	5.17 (2.02)
CXAN	CH_3CN 800 °C/3 h + HT	9.16	1602 (730)	1.06 (0.31)	3.63 (1.60)

[a] Values in parentheses are micropore surface area. [b] Values in parentheses are micropore volume. [c] Hydrogen uptake capacity at -196 °C and 20 bar. [d] Values in parentheses are hydrogen uptake capacity at -196 °C and 1 bar.

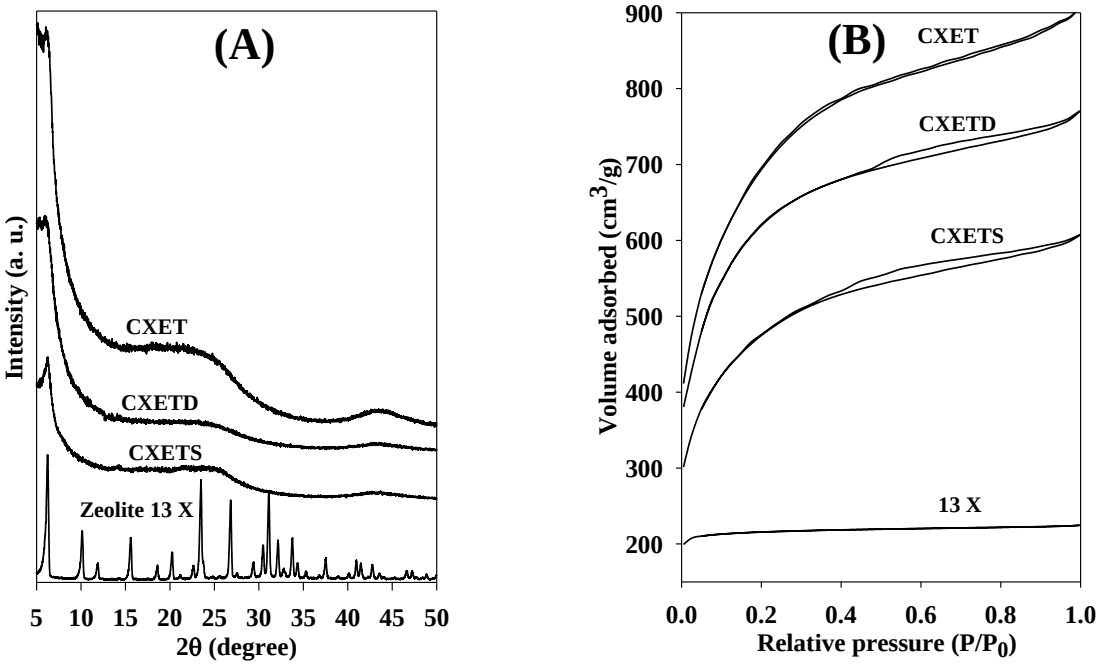

Figure 1. Powder XRD patterns (A) and nitrogen sorption isotherms (B) of microporous carbon templated from zeolite 13X under various conditions via CVD with ethylene as carbon precursor.

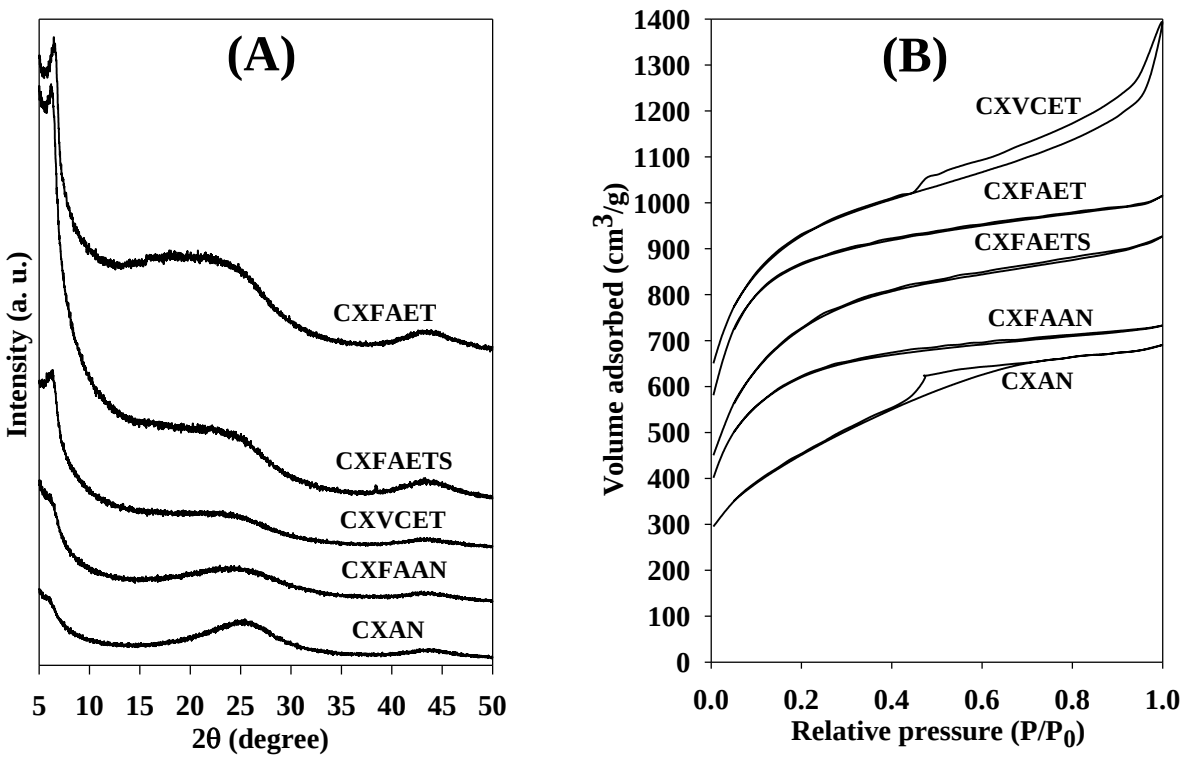

Figure 2. Powder XRD patterns (A) and nitrogen sorption isotherms (B) of microporous carbon templated from zeolite 13X under various conditions by combination of liquid impregnation with furfuryl alcohol and CVD with ethylene. For clarity, the isotherms for sample CXFAET and CXVCET were offset by 50 and 200 along the y axis, respectively.

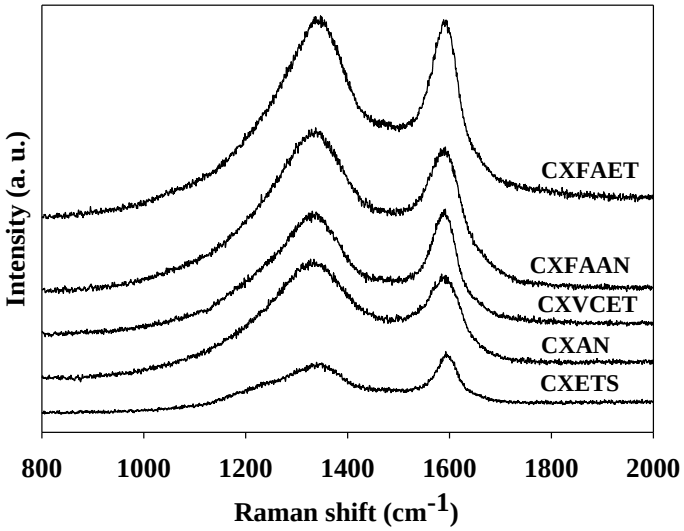

Figure 3. Raman shifts of microporous carbon materials templated from zeolite 13X under various synthesis conditions.

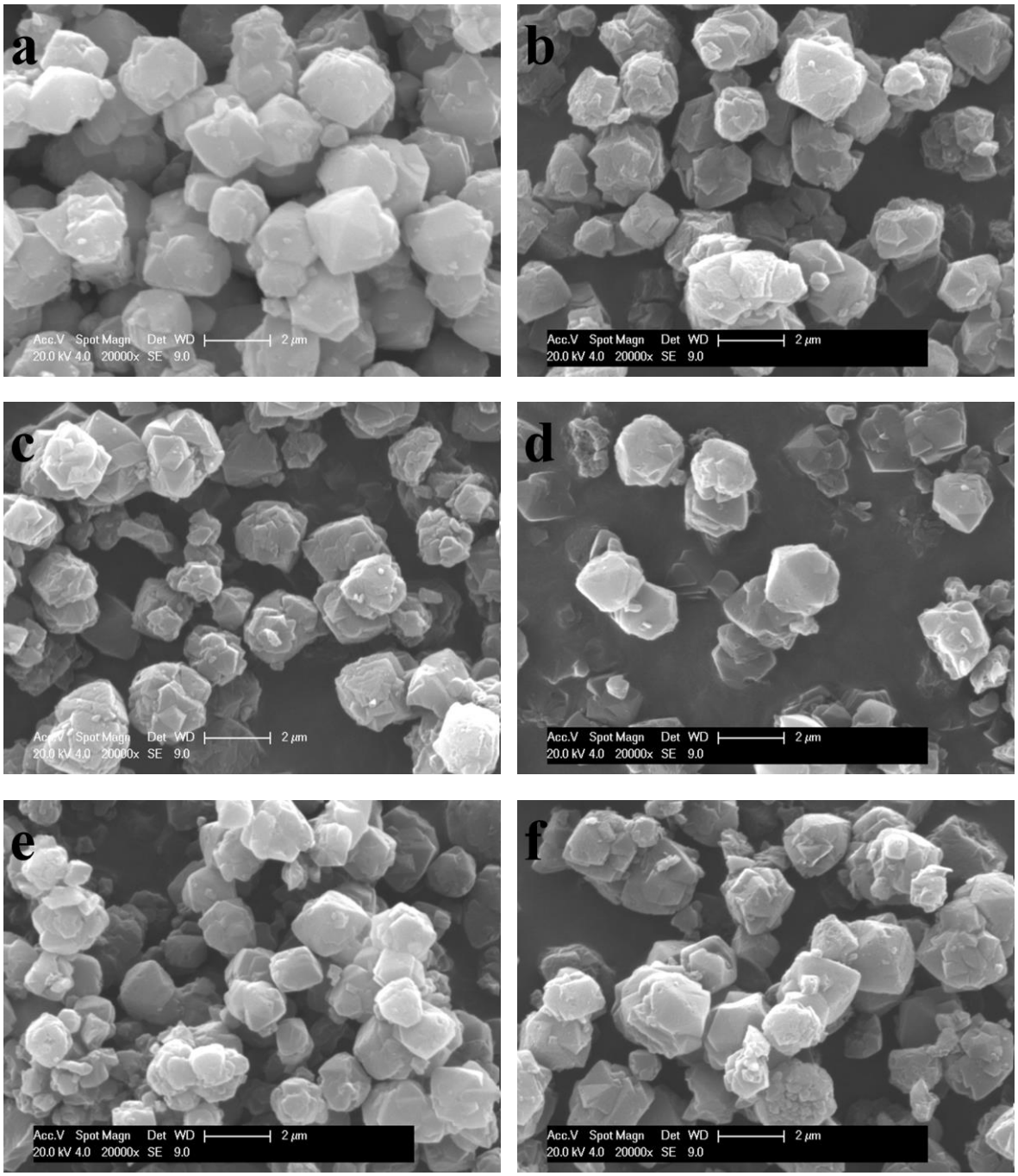

Figure 4. Representative SEM images of microporous carbon materials (b-f) templated from zeolite 13X (a) under various synthesis conditions; (b) CXETD, (c) CXET, (d) CXFAET, (e) CXFAAN and (f) CXVCET.

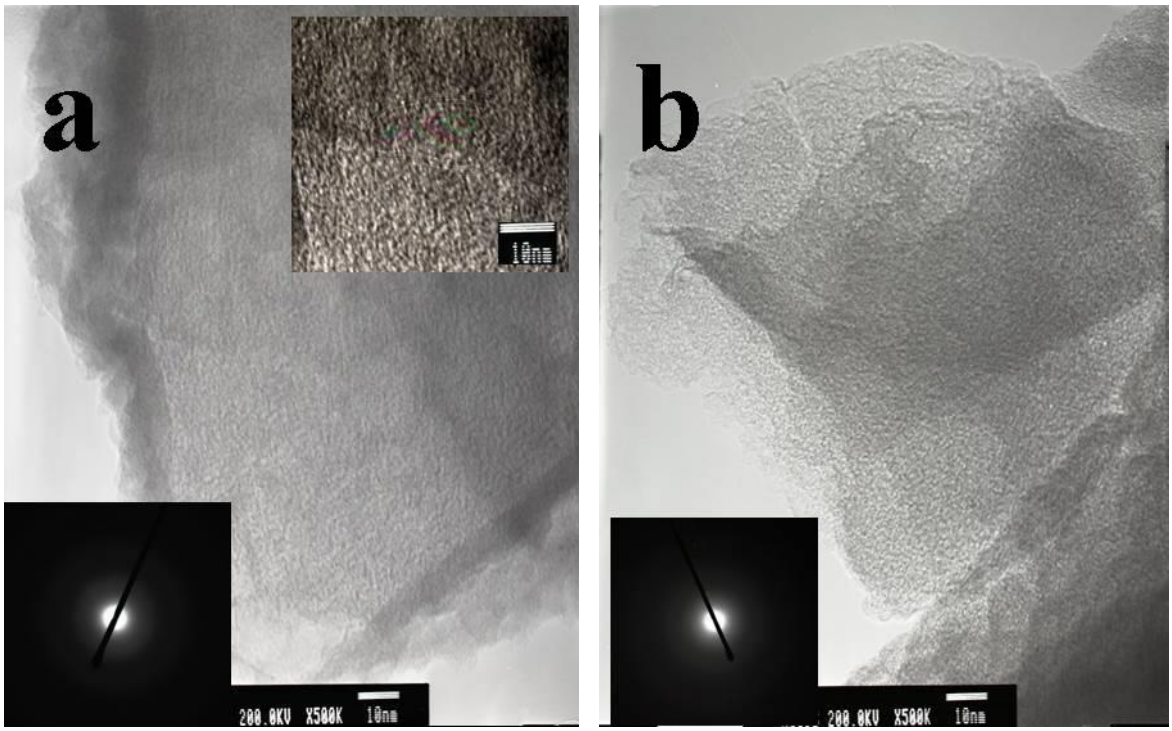

Figure 5. Representative TEM images of microporous carbon materials templated from zeolite 13X. (a) CXET and (b) CXFAET.

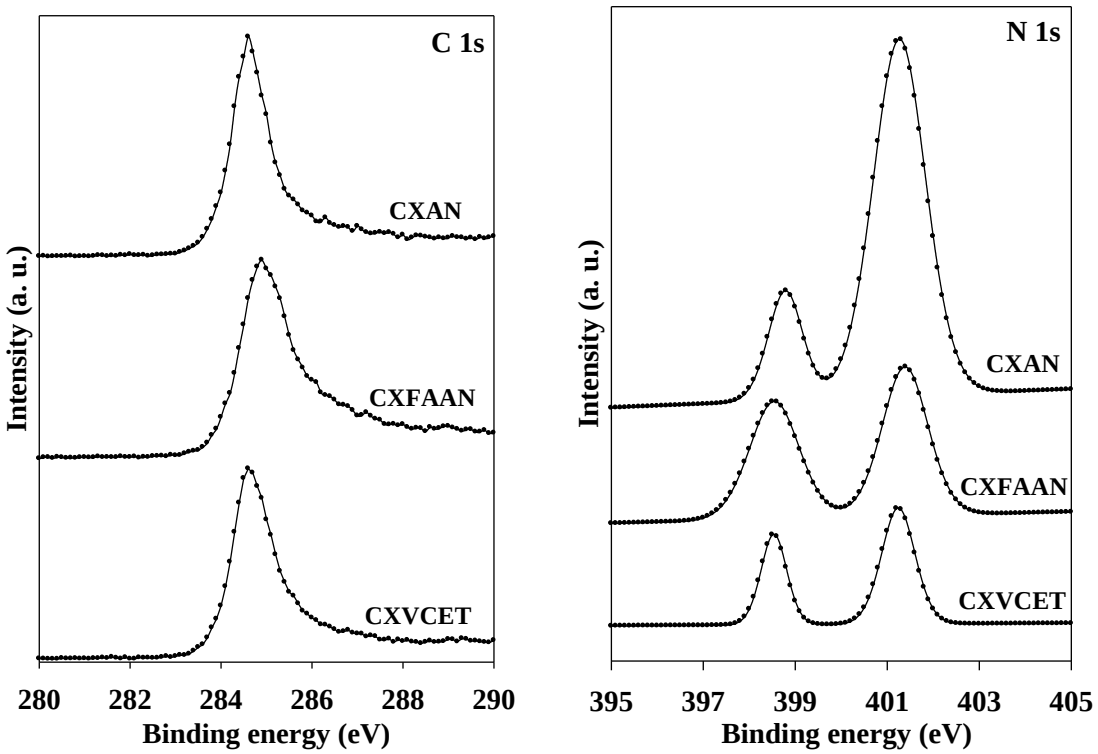

Figure 6. XPS of C1s and N 1s of microporous carbon materials templated from zeolite 13X under various preparation conditions.

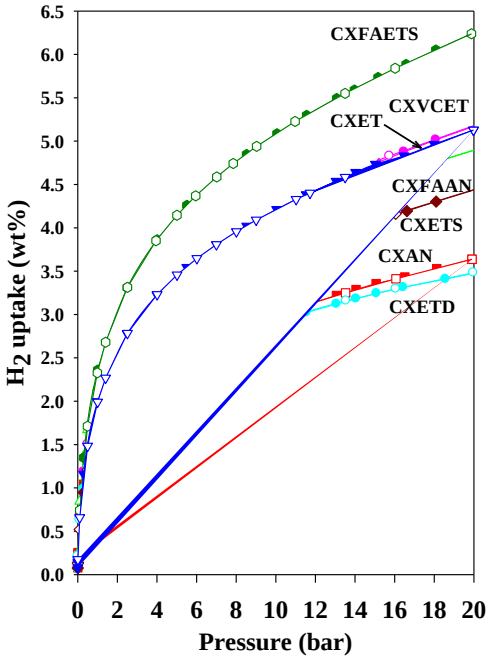

Figure 7. H_2 uptakes of microporous carbon templated from zeolite 13X under various preparation conditions.

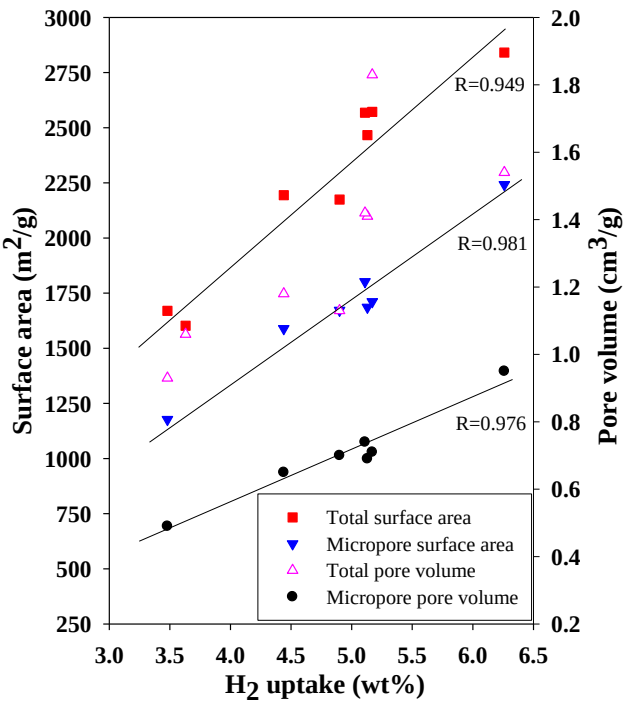

Figure 8. Hydrogen uptake capacities of zeolite 13 templated carbon materials as a function of total surface area, micropore surface area, total pore volume and micropore volume.

Table of content

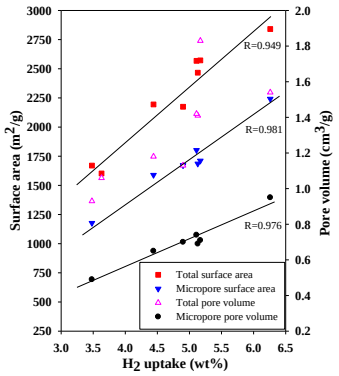

A systematic study on the CVD-based strategies for the nanocasting of porous carbon materials with zeolite 13X as template was presented. The resulting carbon materials exhibit hydrogen uptake capacity up to 6.3 wt%. A linear relationship between the uptake capacity and the total surface area, the micropore volume, and the micropore surface area respectively is found.

Graphical Material

Click here to download Graphical Material Fig 4a.jpg

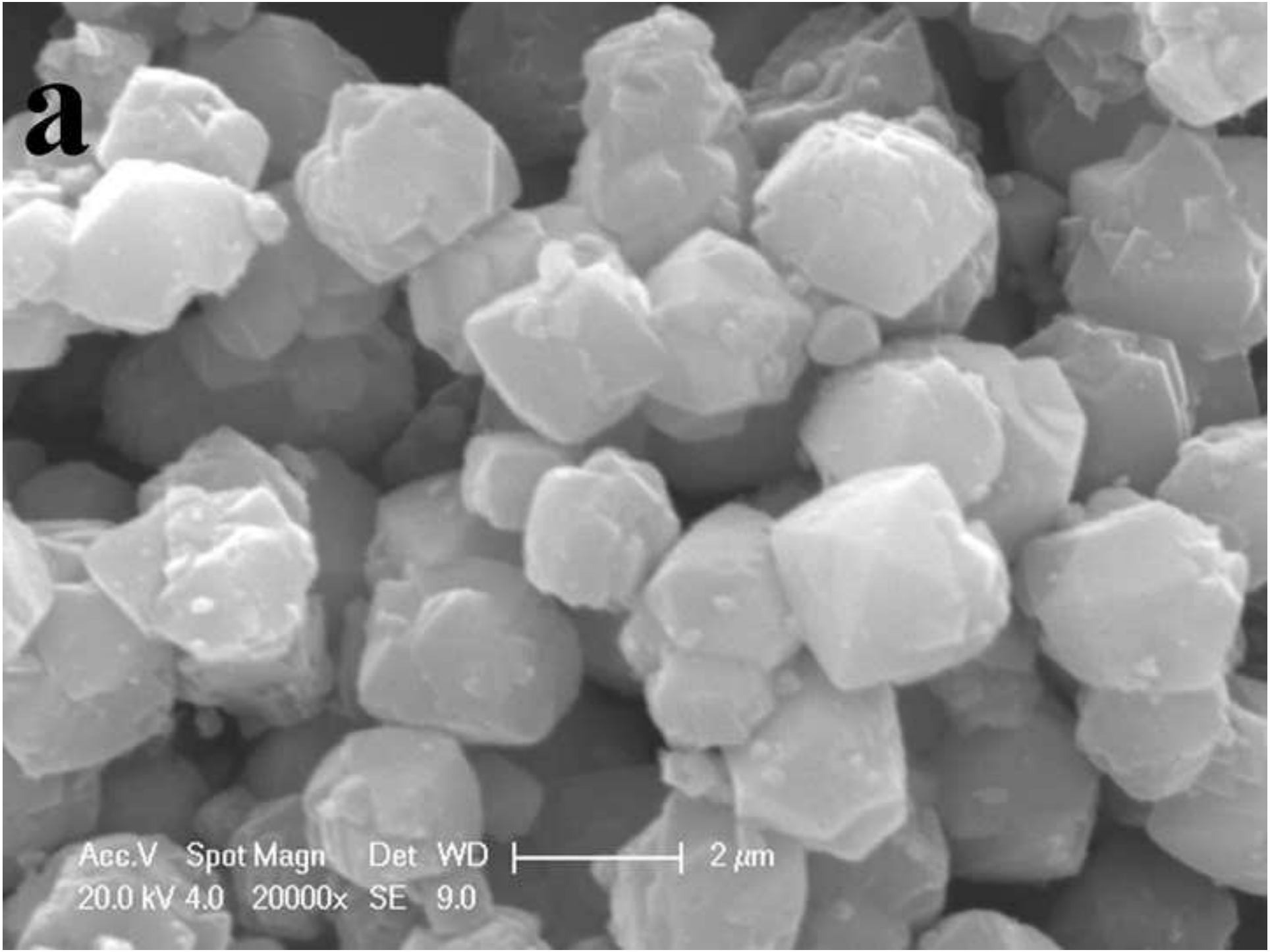

Graphical Material

Click here to download Graphical Material Fig 4b.jpg

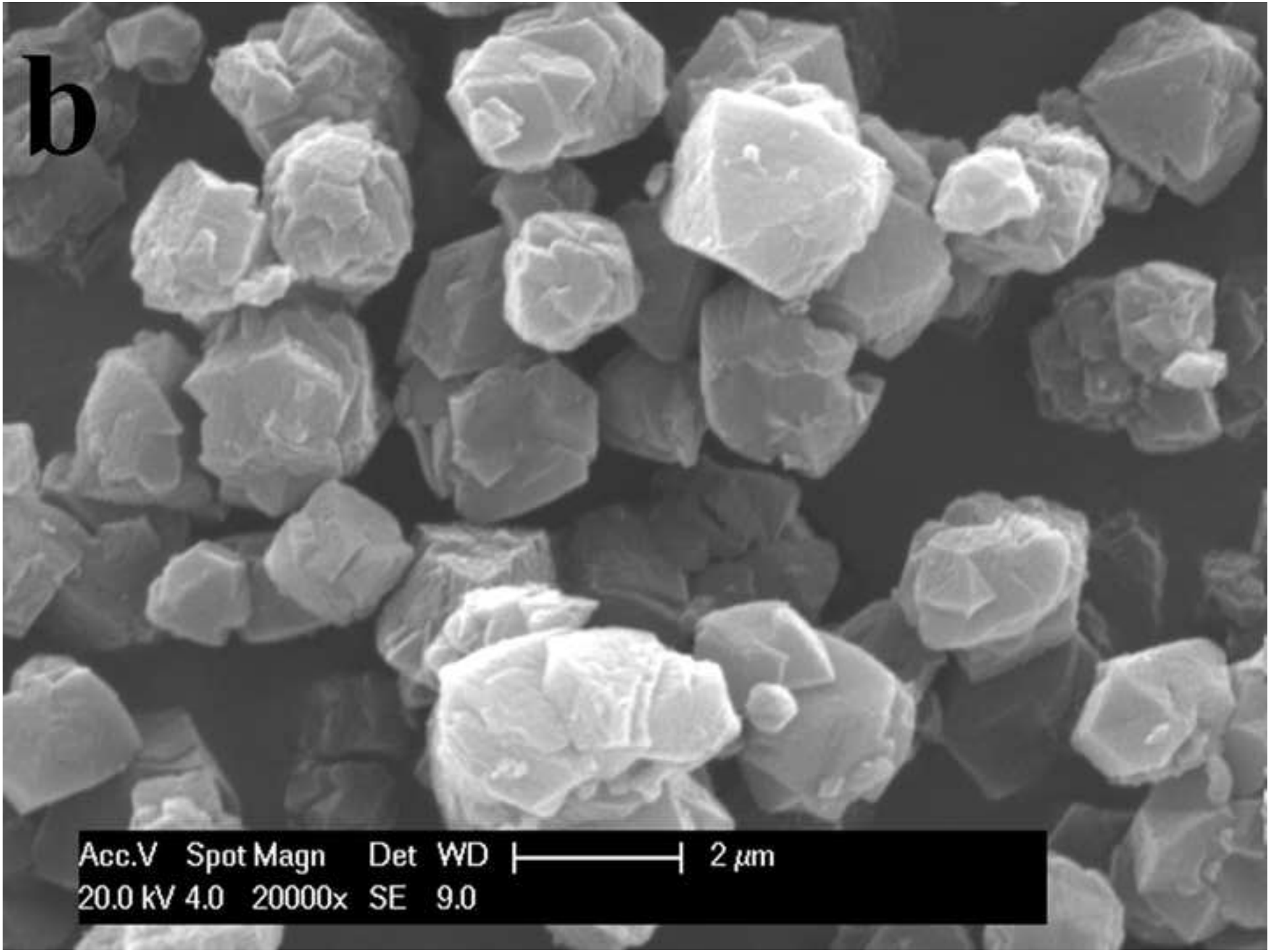

Graphical Material

Click here to download Graphical Material Fig 4c.jpg

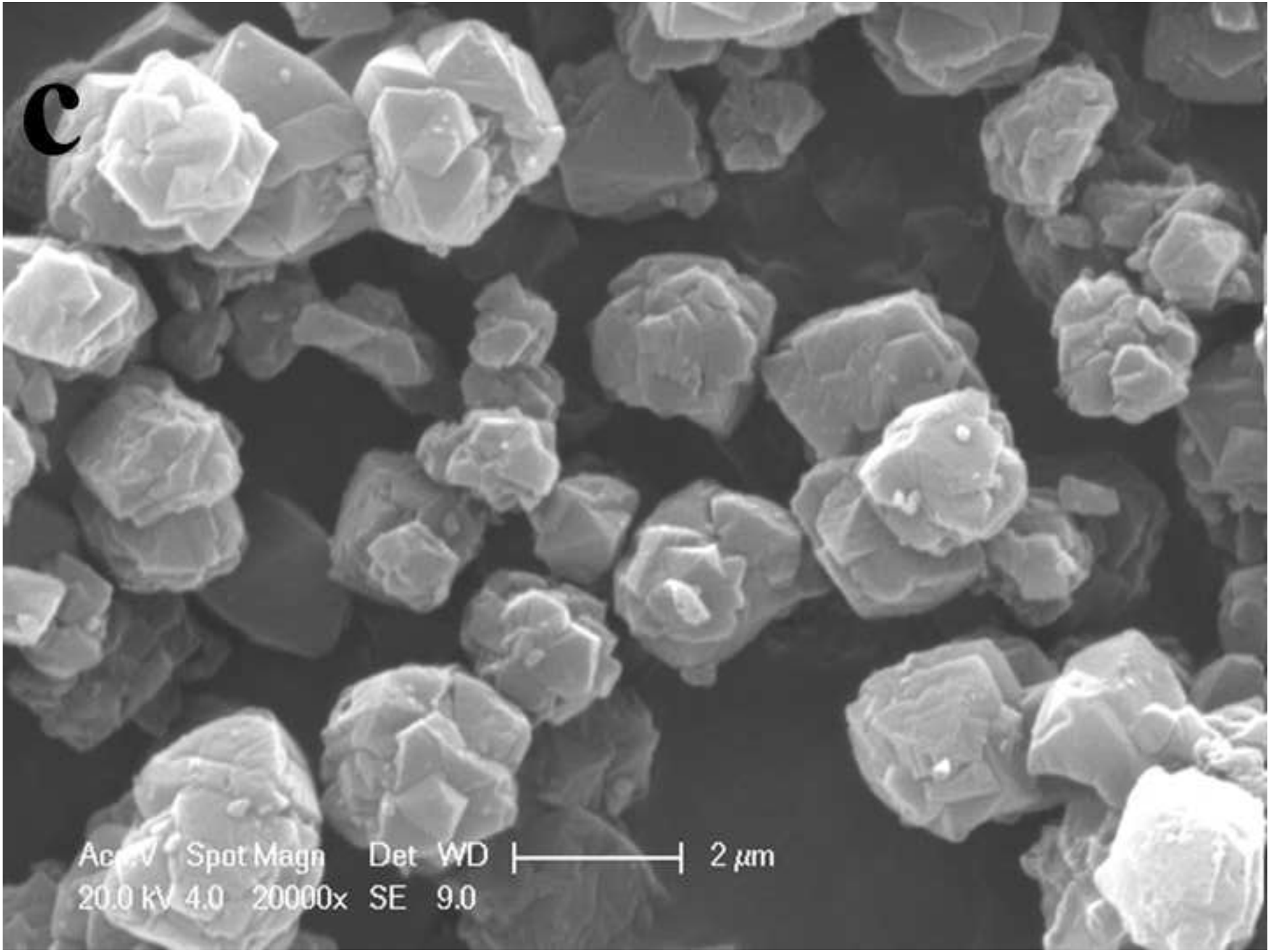

Graphical Material

Click here to download Graphical Material Fig 4d.jpg

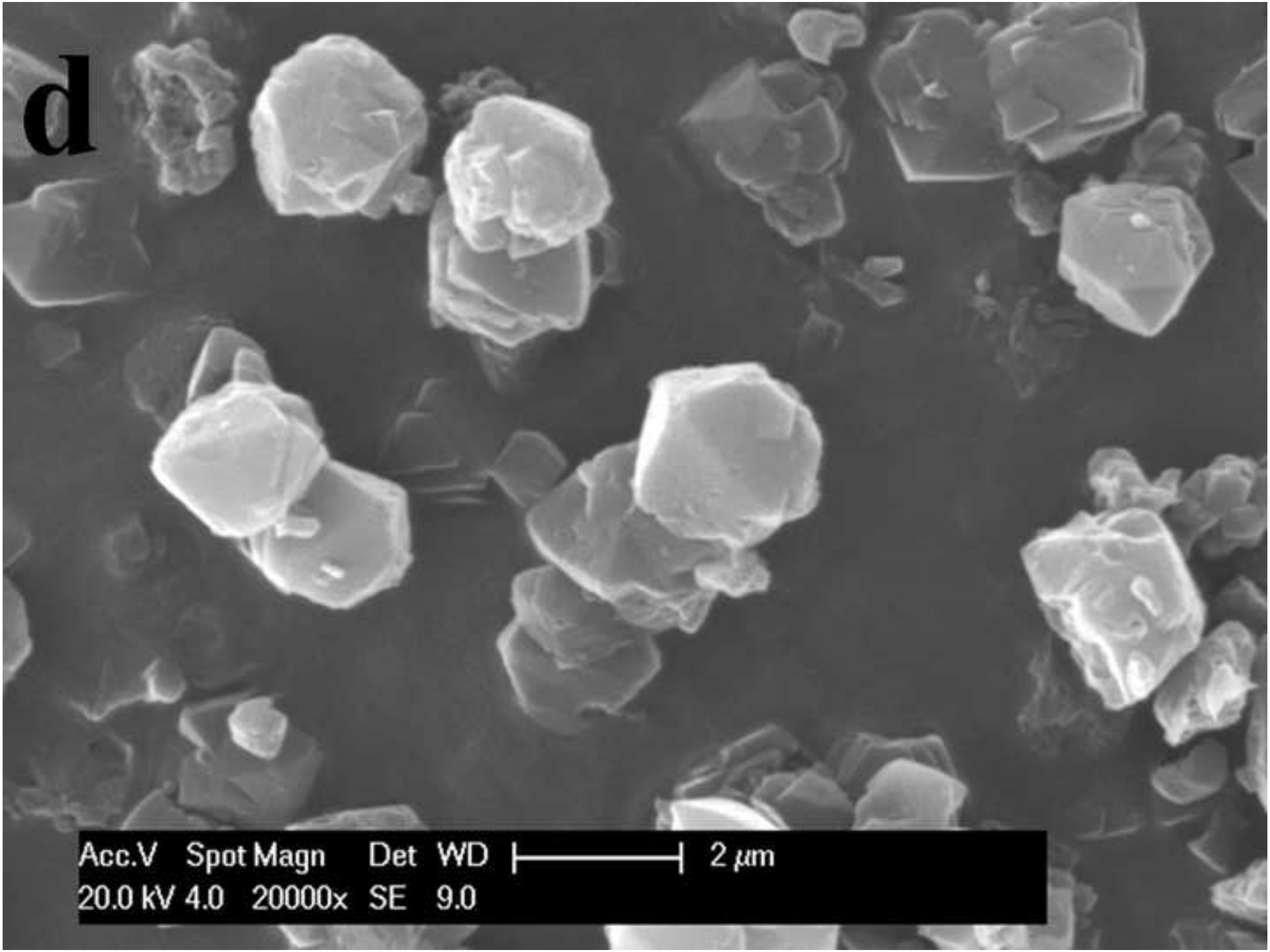

Graphical Material

Click here to download Graphical Material Fig 4e.jpg

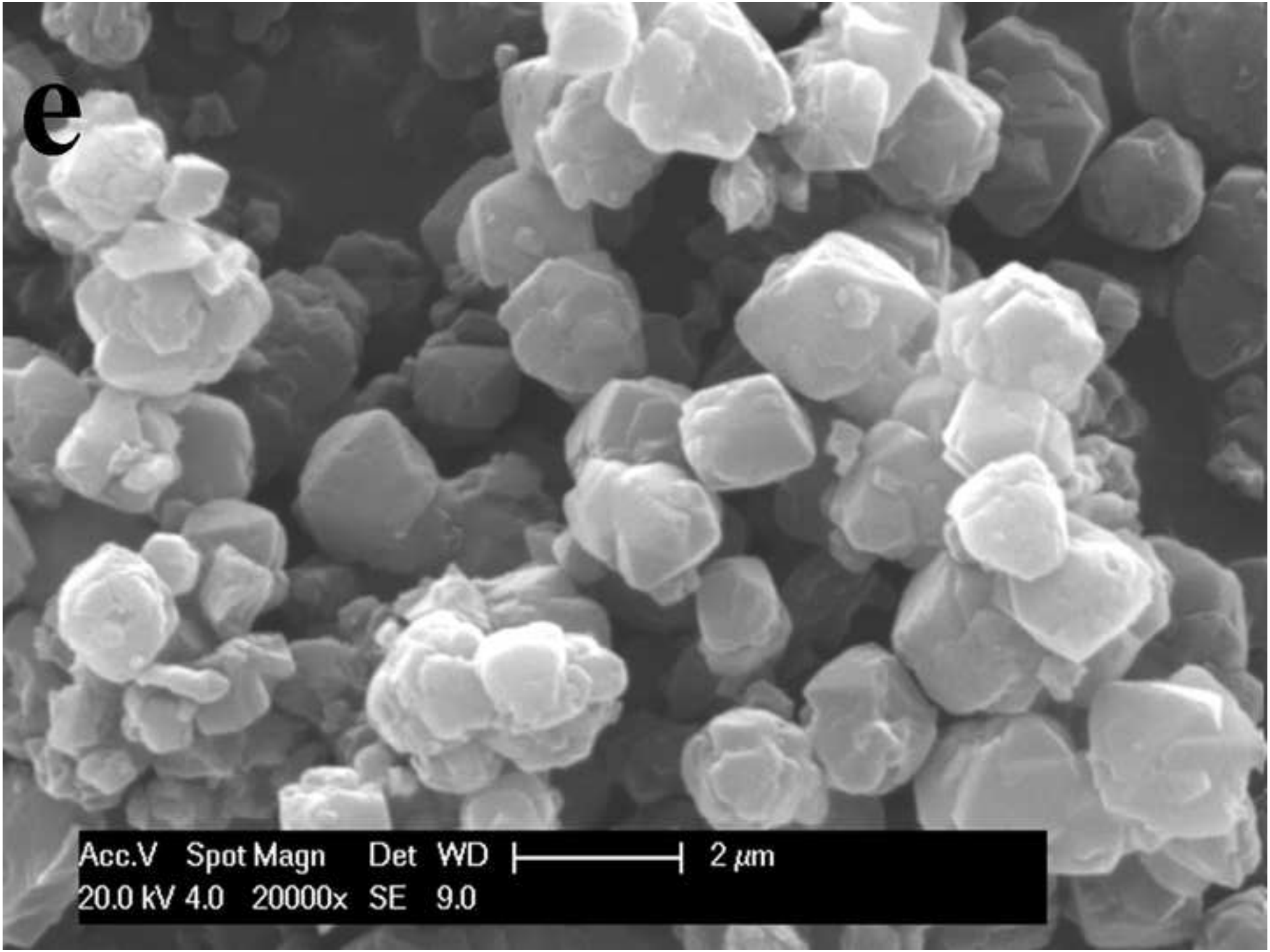

Graphical Material

Click here to download Graphical Material Fig 4f.jpg

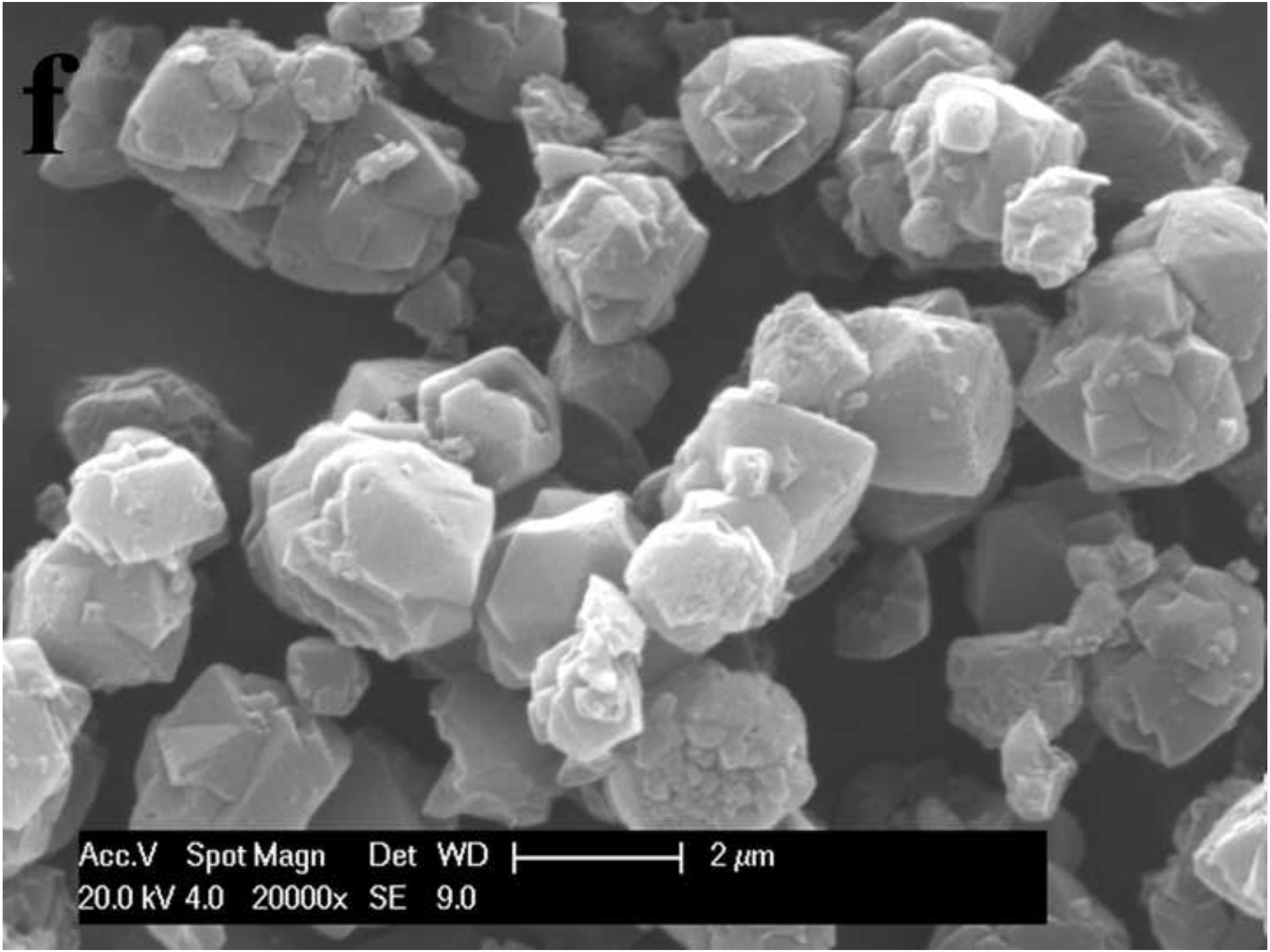

Graphical Material

Click here to download Graphical Material Fig 5a.jpg

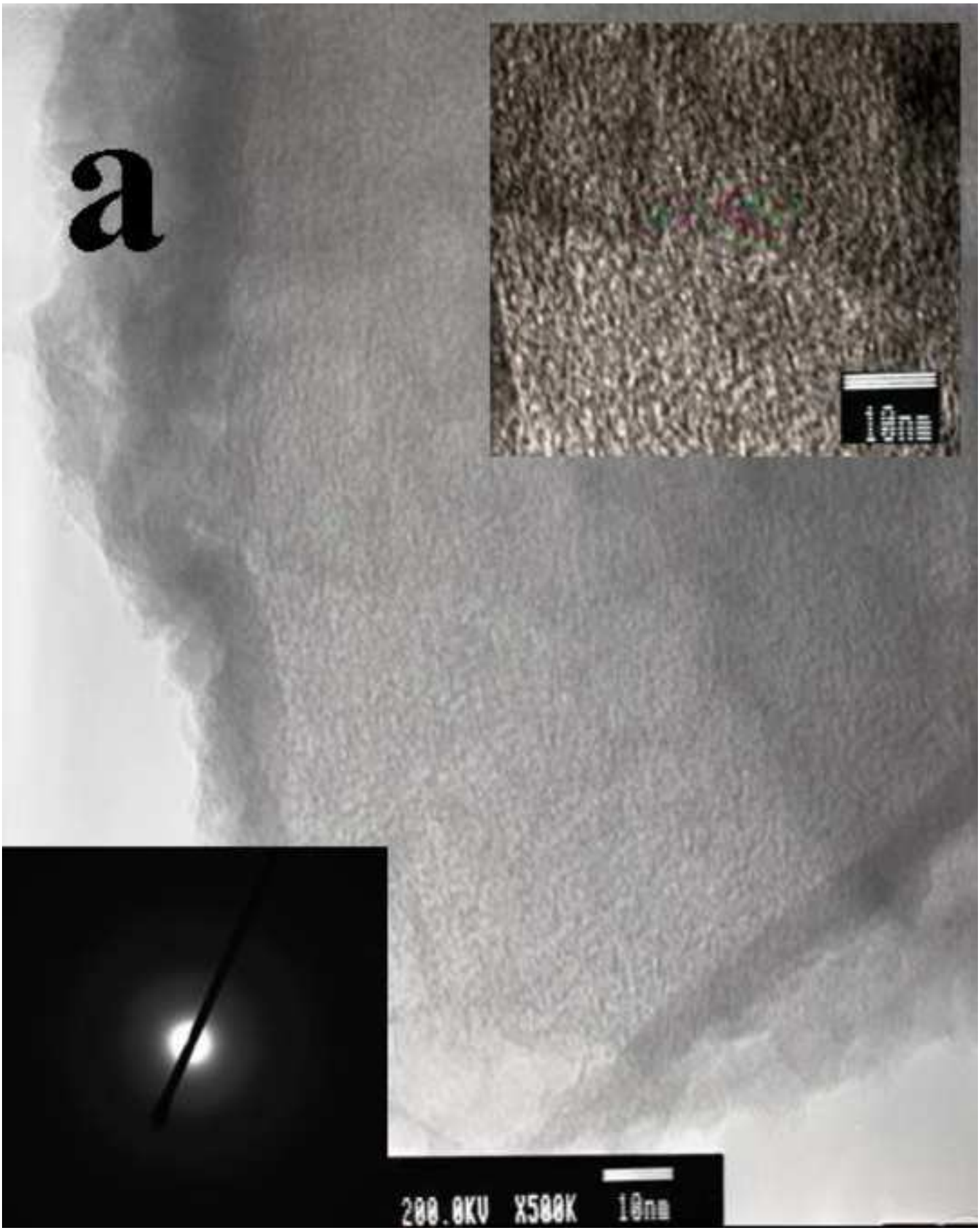

Graphical Material

Click here to download Graphical Material Fig 5b.jpg